

Electron microscopy and structural model of human fibronectin receptor

M.V.Nermut, N.M.Green, P.Eason,
S.S.Yamada¹ and K.M.Yamada¹

National Institute for Medical Research, The Ridgeway, Mill Hill,
London NW7 1AA, UK and ¹National Cancer Institute, NIH,
Bethesda, MD 20892, USA

Communicated by D.A.Rees

Highly-purified human fibronectin receptor (a heterodimer of two distinct subunits, α and β) was studied using electron microscopy and a variety of preparative procedures. It was found that the receptor consists of a globular head ~ 80 by 120 Å and two tails about 20 Å thick and 180 – 200 Å long. The whole complex is ~ 280 Å long. At low concentrations of detergent the receptor forms doublets, triplets or rosettes associated with the tails which possess the transmembrane portion of the molecule. Computer-assisted structure prediction using the published amino acid sequence of both subunits showed differences in the secondary structure of the tails, the α -tail being rich in β -strands, the β -tail having five cysteine-rich repeats analogous to the EGF-like repeats of laminin. Estimates of the length of the tails from the predicted structure conformed well with the dimensions obtained from electron micrographs.

Key words: fibronectin receptor/integrin/electron microscopy/secondary structure

Introduction

A family of receptors for fibronectin and other components of the extracellular matrix, termed integrins, has recently been identified and characterized (see Hynes, 1987; Buck and Horwitz, 1987; Juliano, 1987; Niggli and Burger, 1987; Yamada, 1988; Ruoslahti, 1988 for references). These receptors exist as α – β heterodimers, each of which contains a large external glycosylated portion, a transmembrane domain, and a short cytoplasmic stretch of amino acids at the C terminus. Several integrins have been sequenced, including the β -subunit of the chick 140-kd complex (Tamkun *et al.*, 1986), the α -subunit of the platelet IIb/IIIa complex (Fitzgerald *et al.*, 1987a,b; Poncz *et al.*, 1987), and both the α and β subunits of the human fibronectin receptor (Argaves *et al.*, 1987; Fitzgerald *et al.*, 1987b).

Electron microscopy has been performed on two integrins (Carrell *et al.*, 1985; Parise and Phillips, 1985; Kelly *et al.*, 1987). The major platelet integrin, termed the IIb/IIIa complex, binds to fibrinogen and von Willebrand factor as well as to fibronectin; a chicken gizzard smooth muscle integrin is of as yet unknown ligand specificity. Electron microscopy shows that in both cases the two subunits combine to form an ovoid head with two separated tails (Carrell *et al.*, 1985; Kelly *et al.*, 1987).

We have investigated the morphology of a human integrin receptor that binds specifically to fibronectin, using a variety of electron microscopic preparative procedures. Our data establish the morphology and dimensions of the human fibronectin receptor for comparisons with possible protein domains in the published sequences, and they permit morphological comparisons with two other integrins of broader or unknown ligand specificity.

Results

Electron microscopy

The most informative results were obtained by means of the 'glycerol-spray' technique. However, the type and concentration of detergents substantially influenced the image. In the presence of octyl glucoside (~ 15 mM) a variety of complexes were observed. Figure 1a shows single heterodimers with a rather large head and two tails joined at their ends. More frequent were doublets (Figure 1b), triplets (Figure 1c) or quadruplets (Figure 1d). In very low concentrations of detergent typical rosettes appeared (Figure 1e). These images appear rather similar to those of the platelet IIb/IIIa complex (Carrell *et al.*, 1985) and the gizzard smooth muscle glycoprotein (Kelly *et al.*, 1987).

The two tails could be separated only when 0.1% Triton X-100 was added to the suspension before mixing with glycerol and spraying. A similar effect was obtained with 0.1% sodium dodecylsulphate (Figure 2). The dimensions of the single heterodimer as obtained from rotary shadowed images are shown in Figure 3. Measurements were corrected for the thickness of the tungsten layer by subtracting 30 Å, an average value obtained from several preparations of rotary shadowed DNA. This figure also shows how single complexes appear to form doublets. Although rotary shadowing with pure tungsten provides very fine grain images, exact measurements are not easy at high magnifications (Slayter, 1978) and we therefore refrained from statistical evaluation of the obtained data. However, the length measurements showed very low fluctuation lending credibility to the above figures.

The overall image obtained by negative staining with methylamine tungstate in the presence of 30 mM octyl glucoside was different in the sense that very few doublets, triplets or higher oligomers were observed (Figure 4a). The structures seen most frequently had a round or oblong profile, and their overall average diameter was 95 Å ($n = 610$, $SD \pm 20$ Å). However, a distribution curve clearly showed two peaks suggesting two populations of 'particles', one with an average diameter of about 82 Å, the other 110 Å. They could also represent two different orientations of the molecules: with the tails collapsed on top of the head or underneath the head. This conclusion is supported by low-angle unidirectional shadowing suggesting that the height of the 'round' particles was ~ 70 – 100 Å as opposed to

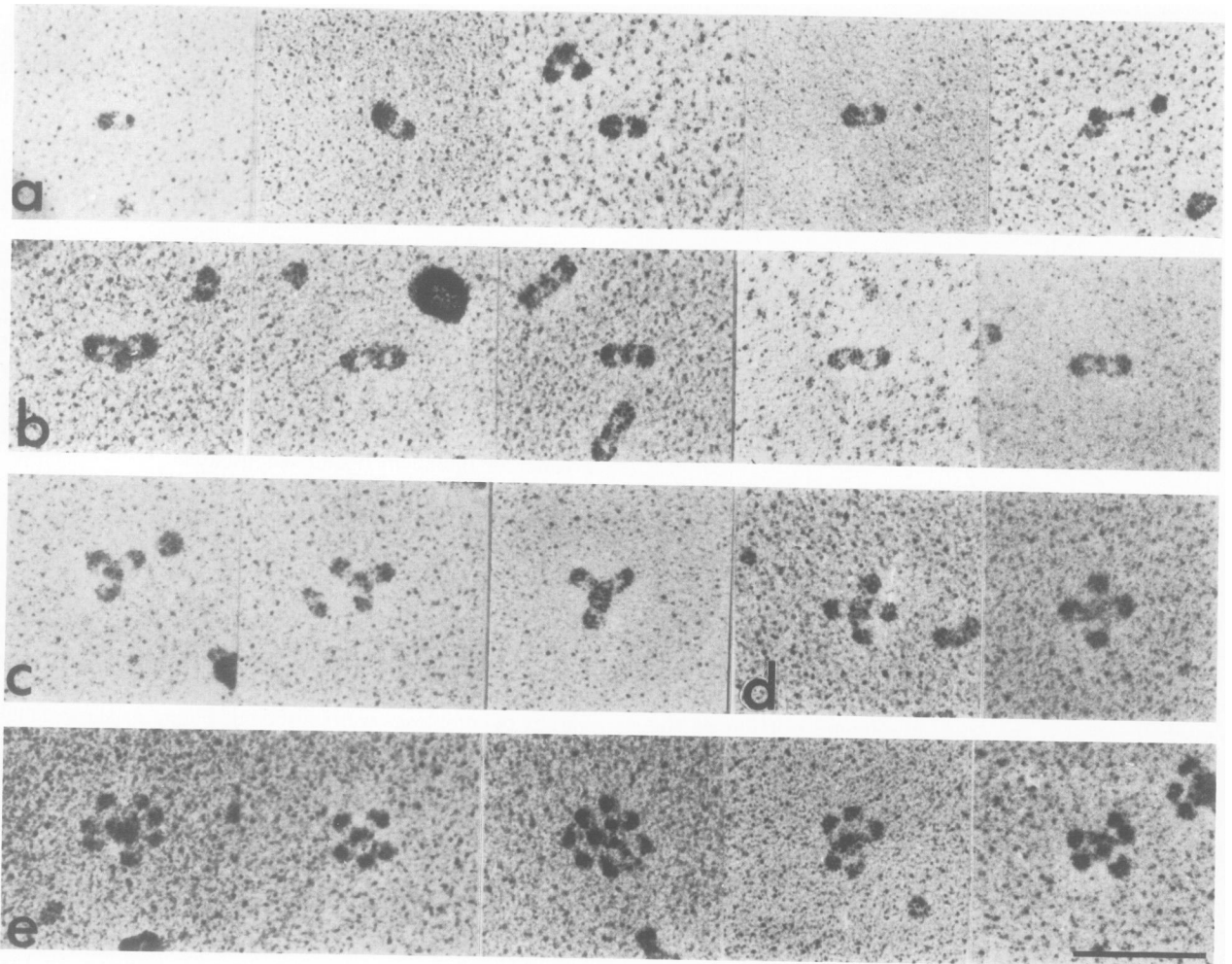


Fig. 1. Gallery of images obtained by rotary shadowing after spraying in 30% glycerol. (a) Single receptor molecules. Note 'single-tail' orientation of receptor on far end; (b) doublets; (c) triplets; (d) quadruplets; (e) rosettes. Bar 100 nm, $\times 180\ 000$.

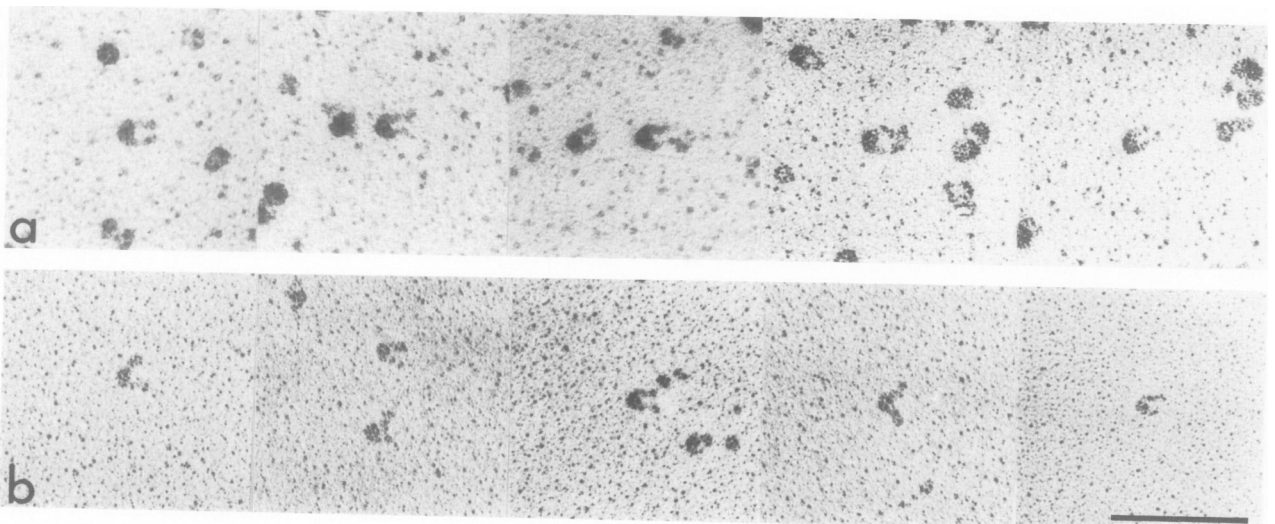


Fig. 2. Single molecules with tails splayed apart by treatment with 0.1% SDS (a) or 0.1% Triton X-100 (b). Note 'hemispherical' heads in some molecules. Glycerol-spray technique, rotary shadowing with tungsten. Bar 100 nm, $\times 180\ 000$.

the overall length of 260–280 Å (Figure 3). No tail-like projections were observed in these preparations. It is obvious that no definite conclusion about the 3-dimensional structure of the head could be made from these pictures; however,

some of the lengthwise oriented molecules displayed a similar head as seen after rotary shadowing (Figures 2a and 4a). Only occasionally have slightly elliptic profiles been observed.

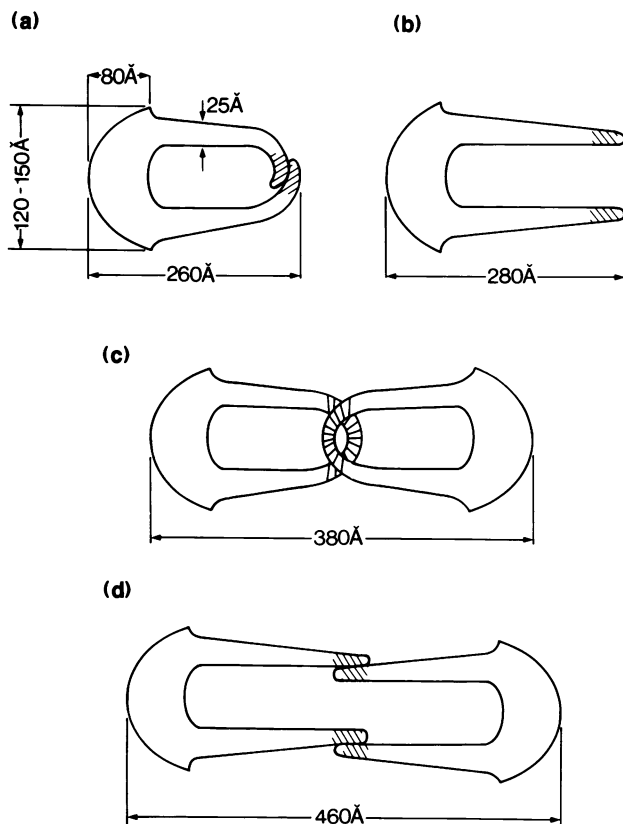


Fig. 3. Diagrammatic representation of fibronectin receptor. (a) Single complex (α - and β -subunits) as seen in low concentration of detergent (e.g. 30-mM octyl glucoside); (b) in higher concentration of detergent (e.g. 0.1% SDS); (c) doublet with hydrophobic portions of tails overlapping; (d) doublet with stretched tails. Dimensions corrected for metal layer.

A certain proportion of macromolecules attached lengthwise. In most cases only one tail was seen in negative stained preparations (Figure 4b), though a few 'two tail' structures could also be identified (Figure 4a). Obviously different orientations of the molecules on the film, e.g. with the two tails superimposed, could account for these two images. The overall length of these molecules was ~ 280 Å. At the end of the tail there was usually a small 'knob' ~ 40 – 50 Å in diameter. This is most probably the result of interaction between the hydrophobic domains of the tails (Figures 3 and 4b).

Rosettes of molecules were also seen after negative staining when the detergent concentration was reduced by extending washing in detergent-free buffer (Figure 4c).

The images observed after freeze-drying or freeze-etching were similar to those obtained by negative-staining. The proportion of lengthwise-oriented molecules was possibly higher, but they were mainly singlets (Figure 5). A few doublets were also present, but no triplets or rosettes as found in Figure 1. The dimensions were in agreement with those obtained by rotary shadowing when corrected for the slightly heavier Pt/C shadowing. Two-tailed structures were very seldom seen in these preparations, suggesting that glycerol infiltration of the receptor suspension in the presence of higher concentrations of detergents helps to keep the tails separated.

The absence of doublets, triplets, etc. after freeze-drying or -etching could be accounted for by the difference in the

preparation conditions. In the case of glycerol spraying the protein suspension is diluted with glycerol to ~ 15 -mM octyl glucoside before spraying, whereas for freeze-drying or -etching the washing takes place after the adsorption of molecules (from 30-mM octyl glucoside) to the carbon film which might prevent the association of molecules into the observed 'oligomers'.

Secondary structure prediction

We correlated the published amino acid sequences with the structure observed in the electron micrographs by taking the transmembrane hydrophobic segments as reference points. The narrow segments that connect the main fibronectin-binding domains to the membrane must from their dimensions correspond to the 200–300 amino acid residues (Green, 1969) on the N-terminal side of the hydrophobic regions. In the β -subunit, a segment of 263 residues includes five cysteine-rich segments (Tamkun *et al.*, 1986; Argraves *et al.*, 1987) separated from the hydrophobic region by a 50-residue segment containing seven proline residues. In the absence of obvious alternative markers the N terminus of the cysteine-rich region is a likely site for the boundary between globular region and tail.

The first four segments are clearly homologous with almost identical spacings between the eight cysteines, several conserved glycines and a general abundance of polar, bend-promoting residues (G,P,N,S,T,R,D,Y, Figure 6). The fifth segment has similar general characteristics but no exact alignment is possible. Comparison with integrin β -subunits from other sources (Law *et al.*, 1987) shows that all the cysteines, including those in the fifth segment, are conserved. The glycines are also quite well conserved, although the overall identity was $< 50\%$. Clearly, the cysteine residues are of vital importance in maintaining the structure and since they are extracellular it is almost certain that they form a stabilizing network of disulphide bonds.

The short arms of laminin provide a precedent for rod-like structures formed from tandem repeats of cysteine-rich segments (Sasaki *et al.*, 1987; Engel and Furthmayer, 1987). It was proposed that the two rod-like segments of each short arm were formed from either five or eight repeats of a 50-residue unit containing eight cysteines and rich in polar, bend-promoting residues. This unit was significantly similar in sequence to epidermal growth factor, homologues of which are known to contribute tandem repeats to other receptor related proteins (Doolittle *et al.*, 1986).

The comparison of the laminin repeats with those of fibronectin receptor β -subunit (Figure 6) shows a significant resemblance to the C-terminal halves of the first four segments. Although the overall sequence homology is not high and there is no clear case for evolution from a common ancestor, it is clear that the tail of the β -subunit and the short arm of laminin could be structurally related. In laminin eight repeats account for ~ 160 Å of the length of the short arm (Engel and Furthmayer, 1987). The five repeats of the β -subunit together with the 50 residues separating them from the membrane could account for 120–140 Å of the stalk. This is in reasonable agreement with the data obtained from electron micrographs (Figures 3 and 7).

The structural correlations of the α -subunit are less clear. The predicted secondary structure of the large globular region (Garnier *et al.*, 1978) consists mainly of β -strands and unstructured regions, but following residue 580 there

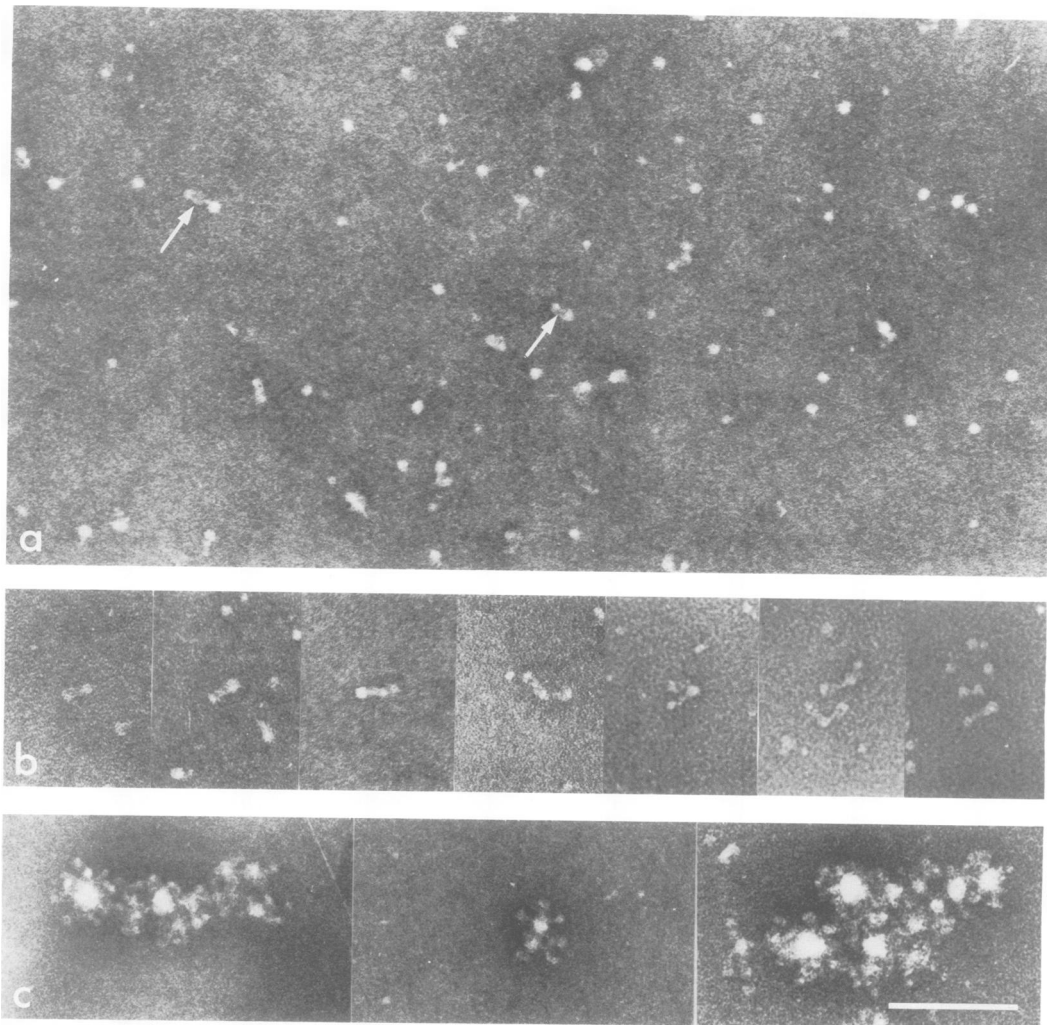


Fig. 4. Fibronectin receptor after negative staining with methylamine tungstate. (a) Overall view of the field. Lengthwise oriented molecules are labelled. (b) Gallery of lengthwise oriented molecules. (c) Gallery of rosettes. Bar 100 nm, $\times 180\ 000$.

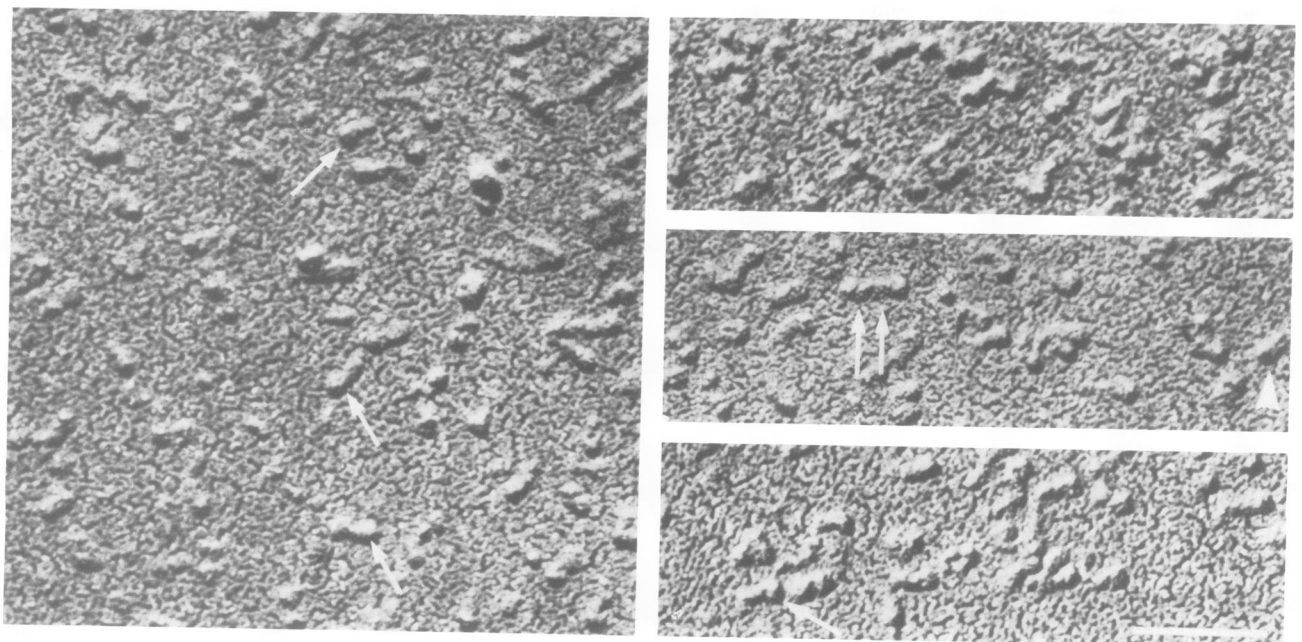


Fig. 5. Fibronectin receptor freeze-etched in the presence of 30-mM octyl glucoside. Unidirectional shadowing with Pt/C, reversed print. Some lengthwise attached molecules are labelled. Bar 100 nm, $\times 180\ 000$.

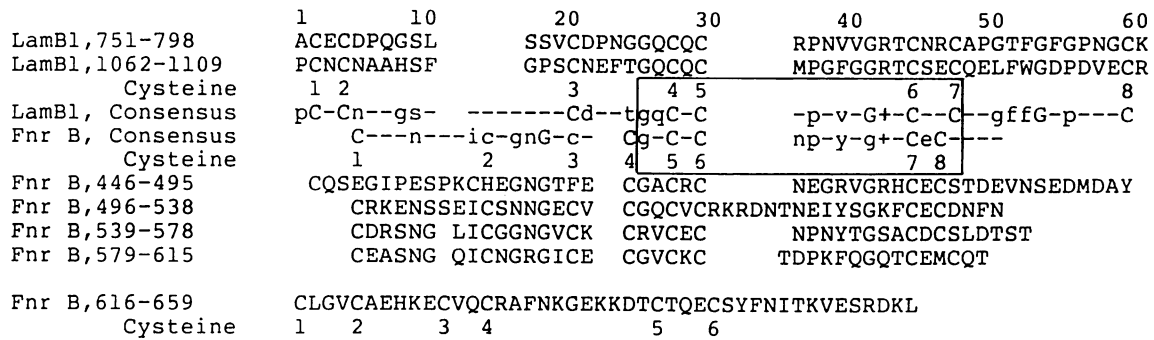


Fig. 6. Alignment of cysteine-rich segments from β -subunit of fibronectin receptor (FnR) and laminin B1 subunit (LamB1). The consensus derived from the first four repeats from FnR is compared with that published by Sasaki *et al.* (1987) for the 13 repeats from laminin. Two individual repeats from laminin are also shown. The fifth cysteine-rich segment from FnR is shown below. In the consensus sequences, lower case residues are partially conserved. The boxed region shows the clearest alignment between the fibronectin receptor and laminin sequences.

are 120 residues in which α -helices predominate. After this point (670), which we suggest as an approximate location for the boundary region, 12 regularly spaced β -strands are predicted bringing us to the cysteine bridge which unites the two halves of the stalk. The final segment (~90 residues) preceding the membrane has an irregular predicted structure and includes 11 residues of proline.

Discussion

The integrins are a remarkable family of transmembrane proteins consisting of two distinct subunits in varying combinations, which interact with each other only by their extracellular glycosylated portions to form a joint head while maintaining two separate tails. Both tails penetrate the plasma membrane and possess small cytoplasmic domains.

The overall morphology of the human fibronectin receptor is similar to that of the platelet GPIIb/IIIa heterodimer which binds to a variety of ligands (Carrell *et al.*, 1985) and of the chicken smooth muscle complex the binding specificity of which is unknown (Kelly *et al.*, 1987). Unlike other authors, we have used a variety of preparative procedures for electron microscopy in an attempt to obtain more accurate data about the dimensions and shape of the complex.

The major problems of electron microscopy of globular macromolecules is their random orientation on the supporting film and the surface tension forces acting during air drying (Nermut, 1982). In our study, negatively-stained preparations of the human fibronectin receptor showed a predominance of 'round' profiles with a very low proportion of molecules attached lengthwise. This on its own would not suffice to build a model of the complex. However, size measurements are more accurate from negatively-stained preparations than from rotary-shadowed ones. On the other hand, the glycerol spray technique appeared rather successful in visualizing the two tails, though many complexes were seen in a variety of orientations. Although we have used the best current method of shadowing we found it difficult to obtain sufficiently accurate measurements at the high magnifications of the prints required. We have therefore combined data from negative staining and rotary or unidirectional shadowing and these are incorporated in the diagram in Figure 7. The agreement with dimensions estimated from amino acid sequences is very good. On the whole, the human fibronectin receptor appears slightly larger than the platelet complex GPIIb/IIIa which has also a lower mol. wt (Carrell *et al.*,

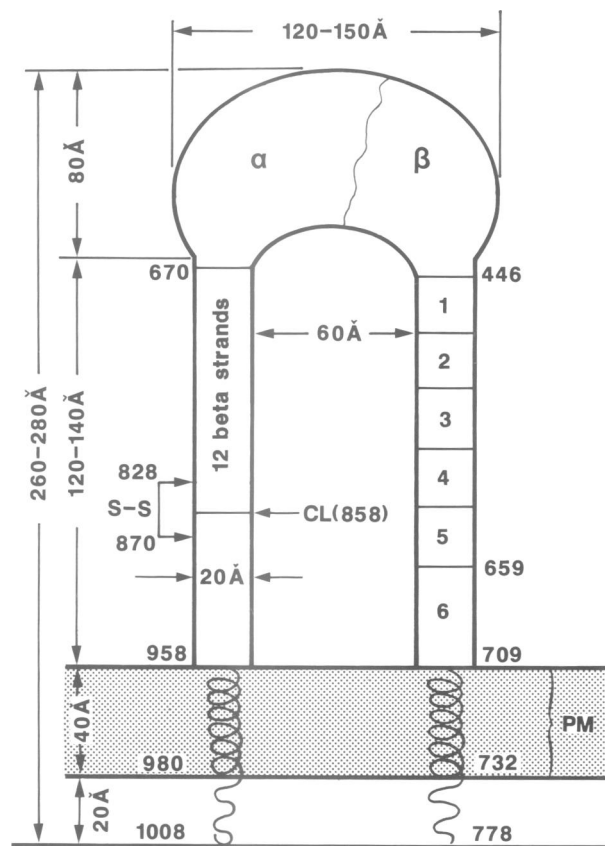


Fig. 7. Structural model for the fibronectin receptor. The sequences were subdivided according to secondary structure and amino acid composition and the subdivisions were correlated with the electron micrographs as indicated in the text. The five cysteine-rich repeats (1-5) would contribute about 100 Å to the stalk if they had the same sequence as in laminin. Together with the short proline-rich segment (6) they could account for most of the extracellular length of the stalk (120-140 Å). There are 12 β -strands in the α -subunit. Figures indicate estimated residue numbers. The overall dimensions represent realistic values obtained from electron micrographs. Approximately in scale. CL, cleavage site; PM, plasma membrane.

1985). Since rotary shadowing does not provide reliable information about the height of structures, we also used unidirectional shadowing in conjunction with freeze-drying or -etching. These methods prevent air-drying artefacts and are an essential complement to the air-dry rotary shadowing methods.

The location of the transmembrane sections at the ends of the tails on both subunits has been clearly documented by associations of two or more single heterodimers where both tails are clearly visualized (Figures 1 and 3). This is consistent with the finding of 20- to 25-residue stretches of hydrophobic amino acids near the C terminus and the location of glycosylation and Ca^{2+} -binding sites in the sequence of the N-terminal domain (Argaves *et al.*, 1987). It was suggested earlier that one of the subunits of the platelet complex has no transmembrane portion and that the other subunit contributes to both tails (Carrell *et al.*, 1985). Our results combined with secondary structure prediction based on recent sequencing are much more consistent with the model depicted in Figure 7. The difference between the predicted secondary structures of the morphologically similar tail segments is very striking. It is not possible to make detailed proposals for the structure of the α -tail, but the structural analogy between the β -tail and the short arms of laminin is significant.

If our model is correct there should be a reasonable correlation between the mol. wt of the complex obtained from the primary structure and the mol. wt calculated from the dimensions. This is relatively simple in the case of the tails, which are close to a slender cylinder ~ 20 Å in diameter and 180 Å long. Using the procedure described by Green (1969) we found that such a cylinder would have a M_r of 39 000. This correlates well with the mol. wt estimated from the number of amino acids (318 amino acids in α -subunit = 35 000, 332 amino acids of β -subunit = 36.5 K). However, there is no obvious geometrical body corresponding to the observed images of the head. We have therefore calculated mol. wt for a hemisphere ($r = 70$ or 80 Å), and prolate or oblate ellipsoids (80:120 Å). The lowest figure (~ 300 K) was found for a prolate ellipsoid, whereas the other two provided figures much above 300 K. Since the total mol. wt of the heterodimer is between 260 and 280 K, the head itself should have only 180–200 K (including carbohydrates). One can conclude that the head of this complex is probably close to a hollow hemisphere or an oblate hemiellipsoid, with an overall shape more closely resembling a mushroom head or a jelly-fish (Figures 2a and 4a). Carrell *et al.* (1985) arrived at a similar conclusion regarding the head of the GPIIb/IIIa complex. However, in contrast to the above integrin, we have not succeeded in separating the subunits of the human fibronectin receptor by treatment with chelating agents such as EDTA or EGTA (unpublished results). Similar experience to this has been reported for a human endothelial membrane integrin-like complex by Fitzgerald *et al.* (1985) and Leeksa *et al.* (1986).

The prediction that the two tails span the plasma membrane with a single α -helix poses a question whether this transmembrane complex would be visualized as intramembranous particles upon freeze-fracturing. The most probable outcome would be that the α -helices would be broken across or alternatively small, ill-defined particles would be present on the external fracture face similar to glycoporphins in red blood cells. However, these would be barely visible in a shadowed replica. Our unpublished experience with EGF-receptor incorporated into lipid vesicles supports the above conclusions. No intramembranous particles could be found in freeze-fracture replicas.

Materials and methods

Purification procedures

The fibronectin receptor used in this study was purified according to an overall approach of Pytela *et al.* (1985) modified as follows. The 110 K cell-binding fragment produced by thermolysin digestion of human plasma fibronectin (Zardi *et al.*, 1985) was coupled to CNBr–Sephacryl (Pharmacia) at a ratio of 10 mg of 100 K fragment per gram of CNBr–Sephacryl. A 50–60 ml column of 110 K–Sephacryl was preceded by a disposable 25 ml Sepharose 4B guard column. The tandem columns were washed with 150 ml of column buffer containing 30-mM octyl- β -D-glucopyranoside (octyl glucoside), Dulbecco's PBS with Ca^{2+} and Mg^{2+} , 1-mM phenylmethylsulphonyl fluoride (PMSF). All solutions were filtered through a 0.22- or 0.45- μm membrane filter. The entire procedure was performed at 4°C.

Human placenta (75 g, cut into 0.5–1 cm² pieces and stored in liquid nitrogen) was partly defrosted and homogenized in a blender in PBS with Ca^{2+} and Mg^{2+} , 10 $\mu\text{g}/\text{ml}$ each of leupeptin and aprotinin, 1-mM PMSF. Octyl glucoside was added to a concentration of 75 mM and PMSF to 3 mM. The homogenate was stirred for 30 min and then centrifuged at 145 000 g for 30 min. The homogenate was loaded on the column at a rate of 150 ml/h with the guard column in place. The column was washed with 300 ml of column buffer at a rate of 200 ml/h. After the coloured homogenate passed the guard column, the guard column was removed from the system and discarded.

The receptor was eluted with 150 ml of 10-mM EDTA, 30-mM octyl glucoside, PBS without Ca^{2+} and Mg^{2+} , 1-mM PMSF at a rate of 150 ml/h. Ca^{2+} was added back to the fractions to 1 mM.

The column was washed with 175 ml of 6 M urea, 1% Triton X-100, PBS with Ca^{2+} and Mg^{2+} , 1-mM PMSF and then 175 ml of 1% Triton, PBS with Ca^{2+} and Mg^{2+} , 1-mM PMSF at a rate of 200 ml/h. Collected fractions were analysed on 4–7.5% polyacrylamide–SDS gels and silver stained (Bio-Rad). The column was equilibrated in column buffer, or for long storage in PBS with azide.

The peak fractions from the 110 K column were pooled, concentrated (Centricon 30, Amicon), added to 0.5 ml of a 50% suspension of agarose-bound wheat germ agglutinin (Vector Laboratories) and incubated overnight at 4°C with agitation. The beads were sedimented and washed 6×1 ml with 30-mM octyl glucoside in PBS with Ca^{2+} and Mg^{2+} and 1-mM PMSF.

The receptor was eluted by incubating the beads for 15 min with agitation with 1 ml of 0.5 M *N*-acetyl-D-glucosamine, 30-mM octyl glucoside, PBS with Ca^{2+} and Mg^{2+} , 1-mM PMSF. This was repeated twice. *N*-Acetylglucosamine was removed by dialysis against 30-mM octyl glucoside in PBS with Ca^{2+} and Mg^{2+} and 1-mM PMSF. Further purification was obtained by high-resolution size fractionation using a Superose 6 FPLC column (HR 10/30, Pharmacia); peak fractions were identified by silver staining after SDS gel electrophoresis.

Preparative procedures for electron microscopy

The starting material was at 0.4 mg/ml protein in 30-mM octyl glucoside in PBS with Ca^{2+} and Mg^{2+} and 2-mM PMSF. A variety of preparative procedures were used.

(i) The glycerol spray technique was used as described by Tyler and Branton (1980). Receptor was mixed with glycerol to a final concentration of 40–50 μg protein and 30% glycerol and sprayed onto freshly cleaved mica. Droplets were rotary shadowed (5 – 7°) with pure tungsten evaporated from an electron gun in a Leybold-Heraeus EPA 100 vacuum coating unit. Some preparations were shadowed from one direction (15 or 20°) or two directions after rotating the specimen table by 90 or 180° between evaporations.

(ii) For freeze-drying, fibronectin receptor (20–40 $\mu\text{g}/\text{ml}$) was adsorbed to glow-discharged carbon films in the presence of 30-mM octyl glucoside followed by extensive washing with distilled water. Some grids were fixed in 1% glutaraldehyde for 5 min before washing and freezing in liquid nitrogen. Drying was carried out at -80 to -90°C (Nermut, 1977) in a Balzers' BAF300 freeze-etch unit. Grids were shadowed with Pt/C from 30° or rotary shadowed with tungsten from 5 to 7° .

(iii) Monolayer freeze-etching (Nermut and Williams, 1977) was also used in a few instances. No cryoprotectant was used and the mica/copper sandwich was plunged into liquid propane at a speed of about 3 m/s using a compressed air operated 'plunger'. Fractured mica surface was etched for 1 min followed by unidirectional shadowing with Pt/C (25 or 30°) and carbon replication.

(iv) For negative shadowing, fibronectin receptor was diluted to about 20 $\mu\text{g}/\text{ml}$ with 30-mM octyl glucoside in PBS, adsorbed to glow-discharged

carbon films for 2–4 min, washed on a drop of distilled water for 5 s and negatively stained with 3% methylamine tungstate pH 6.9 or 1% uranyl acetate.

Specimens were observed in a JEM 1200EX electron microscope operating at 80 kV and calibrated with crystalline catalase.

Acknowledgements

We are grateful to Steven Akiyama for use of the 100 K column and to Wen-Tien Chen for placenta. We also appreciate the initiative of Mr G. Chambers in developing our compressed air plunger for rapid freezing.

References

- Argaves, W.S., Suzuki, S., Arai, H., Thompson, K., Pierschbacher, M.D. and Ruoslahti, E. (1987) *J. Cell Biol.*, **105**, 1183–1190.
- Buck, C.A. and Horwitz, A.F. (1987) *Annu. Rev. Cell Biol.*, **3**, 179–205.
- Carrell, N.A., Fitzgerald, L.A., Steiner, B., Erickson, H.P. and Phillips, D.R. (1985) *J. Biol. Chem.*, **260**, 1743–1749.
- Doolittle, R.F., Fong, D.F., Johnson, M.S. and McClare, M.A. (1986) *Cold Spring Harbor Symp. Quant. Biol.*, **51**, 447–455.
- Engel, J. and Furthmayer, H. (1987) *Methods Enzymol.*, **145**, 3–78.
- Fitzgerald, L.A., Charo, I.F. and Phillips, D.R. (1985) *J. Biol. Chem.*, **260**, 10893–10896.
- Fitzgerald, L.A., Steiner, B., Rall, S.C., Jr, Lo, S.-S. and Phillips, D.R. (1987a) *J. Biol. Chem.*, **262**, 3936–3939.
- Fitzgerald, L.A., Poncz, M., Steiner, B., Rall, S.C., Jr, Bennett, J.S. and Phillips, D.R. (1987b) *Biochemistry*, **26**, 8158–8165.
- Garnier, J., Osguthorpe, D.J. and Robson, N.B. (1978) *J. Mol. Biol.*, **120**, 97–120.
- Green, N.M. (1969) *Adv. Immunol.*, **11**, 1–30.
- Hynes, R.O. (1987) *Cell*, **48**, 549–554.
- Juliano, R.L. (1987) *Biochim. Biophys. Acta*, **907**, 261–278.
- Kelly, T., Molony, L. and BurrIDGE, K. (1987) *J. Biol. Chem.*, **262**, 17189–17199.
- Law, S.K.A., Gagnon, J., Hildreth, J.E.K., Wells, C.E., Willis, C.A. and Wong, A.J. (1987) *EMBO J.*, **6**, 915–919.
- Leeksa, O.C., Zandbergen-Spaargaren, J., Giltay, J.C. and van Mourik, J.A. (1986) *Blood*, **67**, 1176–1180.
- Nermut, M.V. (1977) In Hayat, M.A. (ed.), *Principles and Techniques of Electron Microscopy*. Van Nostrand and Reinhold Co., New York, Vol. 7, pp. 79–117.
- Nermut, M.V. (1982) In Howard, C.R. (ed.), *New Developments in Practical Virology*. Alan R. Liss, Inc., New York, pp. 2–58.
- Nermut, M.V. and Williams, L.D. (1977) *J. Microsc.*, **110**, 121–132.
- Niggli, V. and Burger, M.M. (1987) *J. Membr. Biol.*, **100**, 97–121.
- Parise, L.V. and Phillips, D.R. (1985) *J. Biol. Chem.*, **260**, 1750–1756.
- Poncz, M., Eisman, R., Heidenreich, R., Silver, S., Vilaire, G., Surrey, S., Schwartz, E. and Bennett, J. (1987) *J. Biol. Chem.*, **262**, 8476–8482.
- Pytela, R., Pierschbacher, M.D. and Ruoslahti, E. (1985) *Cell*, **40**, 191–198.
- Ruoslahti, E. (1988) *Annu. Rev. Biochem.*, **57**, 375–413.
- Sasaki, M., Kato, S., Kohno, K., Martin, G.R. and Yamada, Y. (1987) *Proc. Natl. Acad. Sci. USA.*, **84**, 935–939.
- Slayter, H.S. (1978) In Hayat, M.A. (ed.), *Principles and Techniques of Electron Microscopy*. Van Nostrand and Reinhold Co., New York, Vol. 9, pp. 175–245.
- Tamkun, J.W., DeSimone, D.W., Fonda, D., Patel, R.S., Buck, C., Horwitz, A.F. and Hynes, R.O. (1986) *Cell*, **46**, 271–282.
- Tyler, J.M. and Branton, D. (1980) *J. Ultrastruct. Res.*, **71**, 95–102.
- Yamada, K.M. (1988) In Mosher, D.F. (ed.), *Fibronectin*. Academic Press, New York (in press).
- Zardi, L., Carnemolla, B., Balza, E., Borsi, L., Castellani, P., Rocco, M. and Siri, A. (1985) *Eur. J. Biochem.*, **146**, 571–579.

Received on July 12, 1988; revised on October 5, 1988